Conformational Equilibrium of N-Myristoylated cAMP-Dependent Protein Kinase A by Molecular Dynamics Simulations

ARTICLE *in* BIOCHEMISTRY · DECEMBER 2012

Impact Factor: 3.02 · DOI: 10.1021/bi301279f · Source: PubMed

6 AUTHORS, INCLUDING:

Alessandro Cembran
University of Minnesota Duluth
42 PUBLICATIONS **1,119** CITATIONS
SEE PROFILE

Larry R. Masterson
Hamline University
32 PUBLICATIONS **635** CITATIONS
SEE PROFILE

Christopher Mcclendon
Pfizer Inc.
21 PUBLICATIONS **1,235** CITATIONS
SEE PROFILE

Gianluigi Veglia
University of Minnesota Twin Cities
173 PUBLICATIONS **3,838** CITATIONS
SEE PROFILE

doi:10.1016/j.jmb.2011.06.034 J. Mol. Biol. (2011) 411, 823–836

Contents lists available at www.sciencedirect.com

Journal of Molecular Biology

journal homepage: http://ees.elsevier.com.jmb

A Myristoyl/Phosphoserine Switch Controls cAMP-Dependent Protein Kinase Association to Membranes

Ece C. Gaffarogullari[1]†, Larry R. Masterson[2]†, Emily E. Metcalfe[1], Nathaniel J. Traaseth[2], Erica Balatri[1], Musa M. Musa[1], Daniel Mullen[1], Mark D. Distefano[1] and Gianluigi Veglia[1,2]*

[1]*Department of Chemistry, University of Minnesota, Minneapolis, MN 55455, USA*
[2]*Department Biochemistry, Molecular Biology, and Biophysics, University of Minnesota, Minneapolis, MN 55455, USA*

Received 4 May 2011;
received in revised form
16 June 2011;
accepted 18 June 2011
Available online
29 June 2011

Edited by M. F. Summers

Keywords:
protein kinase A;
N-myristoylation;
peripheral membrane proteins;
NMR spectroscopy;
lipid bicelles

The cAMP-dependent protein kinase [protein kinase A (PKA)] mediates a myriad of cellular signaling events, and its activity is tightly regulated in both space and time. Among these regulatory mechanisms is N-myristoylation, whose biological role has been elusive. Using a combination of thermodynamics, kinetics, and spectroscopic methods, we analyzed the effects of N-myristoylation and phosphorylation at Ser10 on the interactions of PKA with model membranes. We found that, in the absence of lipids, the myristoyl group is tucked into the hydrophobic binding pocket of the enzyme (*myr-in* state). Upon association with lipid bilayers, the myristoyl group is extruded and inserts into the hydrocarbon region of the lipid bilayer (*myr-out* state). NMR data indicate that the enzyme undergoes conformational equilibrium between *myr-in* and *myr-out* states, which can be shifted byeither interaction with membranes and/or phosphorylation at Ser10. Our results provide evidence that the membrane binding motif of the myristoylated C-subunit of PKA (PKA-C) steers the enzyme toward lipids independent of its regulatory subunit or an A-kinase anchoring protein, providing an additional mechanism to localize the enzyme near membrane-bound substrates.

**Corresponding author*. 321 Church Street Southeast, Minneapolis, MN 55455, USA. E-mail address: vegli001@umn.edu.

† E.C.G. and L.R.M. contributed equally to this work.

Abbreviations used: THF, tetrahydrofuran; PKA, protein kinase A; PKA-C, C-subunit of PKA; AKAP, A-kinase anchoring protein; NMT, *N*-myristoyltransferase; ITC, isothermal titration calorimetry; DSC, differential scanning calorimetry; CD, circular dichroism; CCLS, carbonyl carbon label selective; HSQC, heteronuclear single quantum coherence; TROSY, transverse relaxation optimized spectroscopy; PDB, Protein Data Bank; DMPC, 1,2-dimyristoyl-*sn*-glycero-3-phosphocholine; D7PC, 1,2-diheptanoyl-*sn*-glyero-2-phosphocholine; 1D, one-dimensional; Myr-CoA, myristoyl coenzyme A; TFA, trifluoroacetic acid; ESI-TOF-MS, electrospray ionization time-of-flight mass spectrometry.

Introduction

Protein kinase A (PKA) is a Ser/Thr phosphoryl transferase that transfers the γ-phosphate group of ATP to protein substrates.[1] PKA phosphorylates more than 100 cytoplasmic and membrane-associated targets.[2] The catalytic subunit [C-subunit of PKA (PKA-C)] is a bean-shaped molecule of 350 amino acids, with a highly conserved core spanning residues 40–300.[3] The catalytic activity of PKA-C is tightly regulated in both space and time via binding partners, including the PKA regulatory subunits (R-subunits, which form the inactive holoenzyme), A-kinase anchoring proteins (AKAPs),[4] and the endogenous protein kinase inhibitor.[5] In addition to regulation by other proteins, a cluster of posttranslational modifications at the N-terminus may fine-tune enzyme

activity, regulation, and localization. These modifications include phosphorylation at Ser10, deamidation at Asn2, and myristoylation at Gly1.[6]

Myristoylation of PKA-C implies the covalent linkage of a tetradecanoyl lipid group to the N-terminal Gly1 of the protein catalyzed by *N*-myristoyltransferase (NMT; EC 2.3.1.97). Myristoylation has often been associated with membrane targeting.[7] However, myristoylation may actively participate in protein kinase activation or deactivation. For instance, a myristoyl/phosphotyrosine switch has been proposed as an integral part of the regulatory cycle of the c-Abelson tyrosine kinase,[8] where N-myristoylation modulates the activity of the enzyme by gating the effects of the SH2 domain.[8] In contrast, myristoylation of c-Src kinase has a positive effect on catalytic activity and, together with membrane binding, may regulate enzyme ubiquitination and degradation.[9] Therefore, myristoylation may have varying effects on protein kinase function and may tune different signaling events regulated by these enzymes.

Thermal denaturation studies of myristoylated PKA-C [myr(+)PKA-C] show that N-myristoylation confers higher stability when compared to non-myristoylated PKA-C [myr(−)PKA-C].[10] On the other hand, phosphorylation kinetic experiments with kemptide (a soluble standard substrate) show that the catalytic efficiency of myr(+)PKA-C is indistinguishable to that of myr(−)PKA-C.[10] Comparison of X-ray structures of both mammalian and recombinant PKA-C show that the N-terminus of the protein kinase is essentially disordered in the absence of myristoylation and becomes helical and ordered upon myristoylation.[11] In the crystal structure, the myristoyl group of myr(+)PKA-C is retracted in a hydrophobic pocket of the protein kinase far away from the entrance of the active site.[11] The aliphatic chain of the myristoyl group stretches within this hydrophobic pocket, connecting the large lobe to the small lobe and making contacts with a number of peripheral segments in the enzyme.[10] These segments include the A-helix, the apex of a loop connecting the C-helix with β-strand 4, the E-helix, and the C-terminal tail.[11]

Although biophysical and high-resolution studies offer a view of how stability can be afforded by positioning the myristoyl group within the catalytic core of myr(+)PKA-C, mechanistic data regarding the role of the myristoyl group in substrate recognition and modulation of catalytic function at the membrane interface are still lacking. In fact, localization and structural studies of myr(+)PKA-C in the presence of a lipid membrane are limited to short myristoylated peptides corresponding to the N-terminal portion of the protein kinase (821,[12] 2597[13]). Based on these data, it has been hypothesized that both myristoylation and a basic face of an amphipathic helix at the N-terminus of myr(+)PKA-C steer the enzyme toward the membrane to recognize and phosphorylate membrane-bound substrates.[12] Also, structural disorder induced upon Ser10 phosphorylation in a peptide corresponding to the N-terminus of myr(+)p(+)PKA-C has been proposed as a subsidiary control on the protein kinase to bind lipid membranes.[13] These results are quite intriguing and open up the possibility that membrane association of PKA-C is controlled by a myristoyl/phosphoserine switch.[14] Other reports have proposed the necessity of accessory or regulatory proteins to target myr(+)p(−)PKA-C to the membrane.[15] Specifically, fluorescence data support the role of R-subunit type II to form an isoform-specific switch in myr(+)p(−)PKA-C, which causes it to target cellular membranes.[15] Also, the identification of AKAPs in the role of PKA-C membrane localization[4] has opened new questions regarding the exact functional role of myristoylation. How does the conformation of the myristoylated and phosphorylated PKA-C peptides compare to the full-length enzyme in solution and in the presence of membranes? Could the myristoyl hydrophobic pocket act as an allosteric site?

In this paper, we analyzed the role of N-myristoylation and its structural coupling with Ser10 phosphorylation in the context of lipid membranes for full-length PKA-C. These studies were made possible thanks to homogenously myristoylated samples prepared using *in vitro* site-specific ligation chemistry, which enabled the production of isotopically labeled myr(+)PKA-C for biophysical and structural studies. In this manner, myr(+)PKA-C could be obtained in milligram quantities with or without S10 phosphorylation. Using a combination of isothermal titration calorimetry (ITC), differential scanning calorimetry (DSC), circular dichroism (CD), steady-state kinetics, and NMR spectroscopy, we found a conformational switch in myr(+)PKA-C that is modulated by S10 phosphorylation or membrane interactions. These data confirm the previously proposed mechanism of myr(+)PKA-C interactions with the membrane[15] while offering an atomistic view of the allosteric changes induced by both myristoylation and membrane binding in the enzyme's active site.

Results

Folding, stability, and function of *in vitro* myristoylated PKA-C

The production of recombinantly expressed myristoylated PKA-C has been previously accomplished by co-expression of NMT and PKA-C in *Escherichia coli*

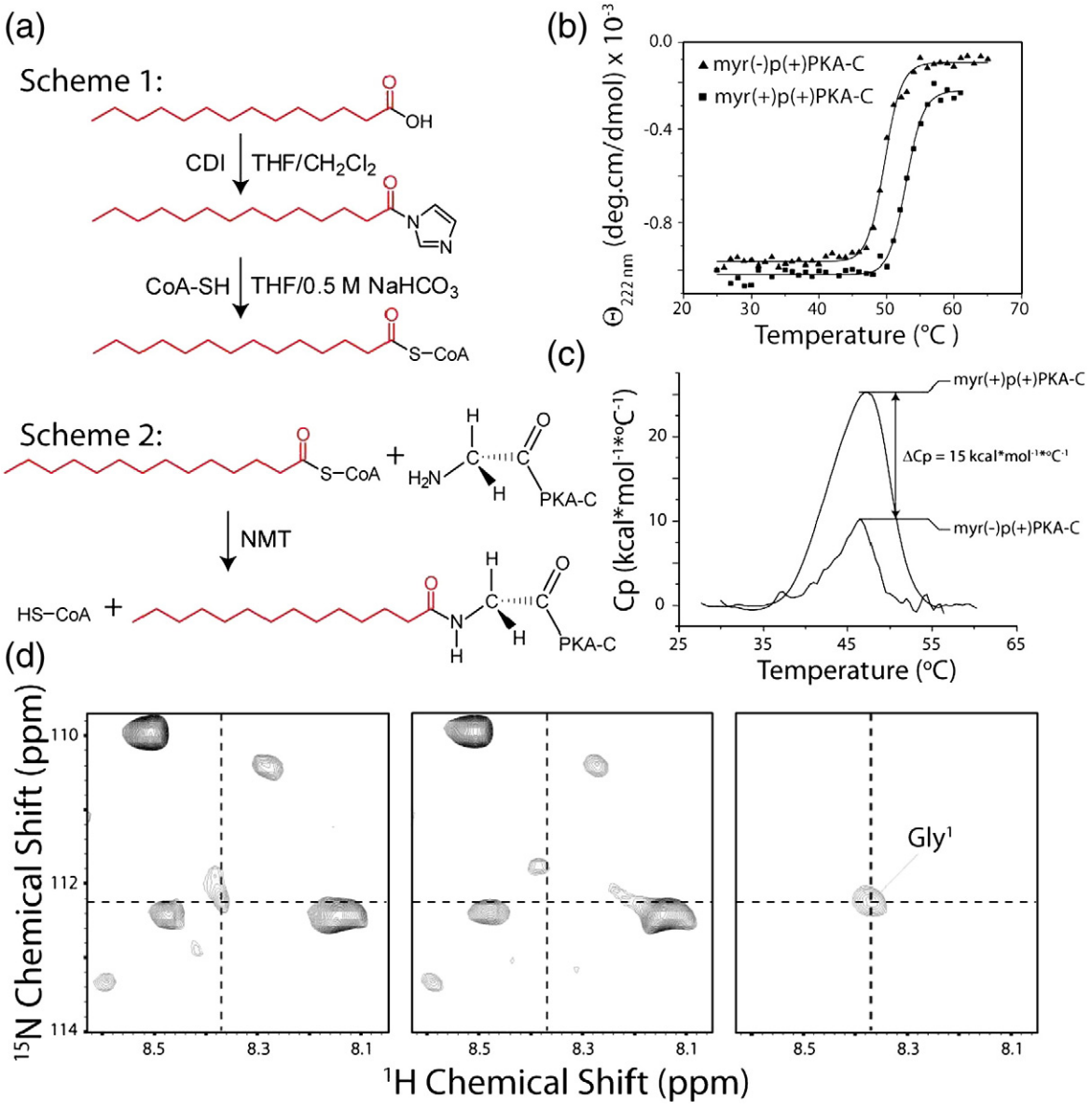

Fig. 1. Preparation and characterization of myr(+)p(+)PKA-C. (a) Synthetic schemes for the preparation of Myr-CoA and myr(+)PKA-C. (b) CD melting curves of PKA-C samples. N-myristoylation increases the enzyme thermostability by ~3 °C. (c) DSC profiles of myr(+)p(+)PKA-C and myr(-)p(+)PKA-C. The difference in the enthalpy of unfolding is ~15 kcal*mol*°C^{-1}, in favor of the myristoylated sample. (d) 2D portions of the [^{1}H/^{15}N]-CCLS-HSQC experiments for the identification of the linkage between the myristic group, labeled at 1-^{13}C, and Gly1. Experimental conditions are detailed on the methods section.

bacteria.[10,16] This procedure results in a mixture of myristoylated PKA-C in two different phosphoisoforms, which are not phosphorylated at S10. In addition, a high level of NMT expression is obtained, which is difficult to separate from the kinase.[17] To avoid the difficulties associated with the separation of this complex mixture and provide an avenue to obtain myr(+)PKA-C with S10 phosphorylated [myr(+)p(+)PKA-C] or unphosphorylated [myr(+)p(−)PKA-C], we optimized a protocol for the myristoylation of myr(−)PKA-C phosphoisoforms *in vitro*. In this manner, we could utilize recombinantly expressed myr(−)PKA-C, which contains phosphorylated or unphosphorylated S10, to test the functional effects of myristoylation and N-terminal phosphorylation on the full-length enzyme.

First, we synthesized myristoyl coenzyme A (Myr-CoA) according to a previously published protocol (Fig. 1a).[18] Then, we carried out NMT-catalyzed myristoylation by adding Myr-CoA to myr(−)p(+)PKA-C or myr(−)p(−)PKA-C. The protocol required an extensive optimization of the experimental

Table 1. Kinetic and thermodynamic parameters of myr(+)p(+)PKA-C and myr(−)p(+)PKA-C

	myr(−)p(+)PKA-C	myr(+)p(+)PKA-C
Molecular mass (a.m.u.)	40,685	40,896
K_m (μM)[a]	40 ± 9	41 ± 3
V_{max} (μM/s)[a]	0.20 ± 0.02	0.21 ± 0.01
k_{cat} (s^{-1})[a]	20 ± 2	21 ± 1
K_d^{ADP} (μM)	20.1 ± 4.0	24.1 ± 0.4
T_m (°C)	49.7 ± 0.1	52.9 ± 0.1

[a] Steady-state kinetic measurements were performed with the standard soluble substrate kemptide.

conditions by testing different detergents that would retain the solubility of the myristoylated product during the enzymatic reaction. However, since low nanomolar concentrations of NMT are sufficient for full myristoylation, isolation of the myristoylated product is more facile. After the reaction, the myristoylated product was separated from residual non-myristoylated PKA-C (less than ~2%) by ion-exchange chromatography. The efficiency of the *in vitro* myristoylation of PKA-C was found to be >98% based on analytical HPLC or standard addition monitored by electrospray ionization time-of-flight mass spectrometry (ESI-TOF-MS).

The covalent attachment of the myristoyl group to PKA-C and subsequent changes in the physical properties of the enzyme were confirmed by (1) ESI-TOF-MS, (2) thermal melting, and (3) NMR spectroscopy. For myr(+)p(+)PKA-C, the mass spectrum of the purified product is shifted by an additional 211 a.m.u. (corresponding to the myristoyl group; Fig. S1 and Table 1). The CD spectra of myr(−)p(+)PKA-C and myr(+)p(+)PKA-C showed the same profile (Fig. S2), consistent with the small structural changes observed by X-ray crystallography.[6] However, thermal melting (T_m) monitored by CD spectroscopy showed an increase of 3.2 °C for myr(+)p(+)PKA-C over myr(−)p(+)PKA-C (Fig. 1b), as shown previously for recombinantly expressed myr(+)p(−)PKA-C.[10] This was further verified by DSC, which revealed a ΔC_p of ~15 kcal/mol between myr(+)p(+)PKA-C and myr(−)p(+)PKA-C and a shift of ~3 °C in melting point (Fig. 1c).

The N-terminal covalent attachment of the myristoyl group in myr(+)p(+)PKA-C was confirmed by NMR spectroscopy. Specifically, we used the [^{1}H/^{15}N]carbonyl carbon label selective (CCLS)–heteronuclear single quantum coherence (HSQC)[19] on a myr(+)p(+)PKA-C sample, which contained uniform ^{15}N labeling and ^{13}C labeling only at the C-1 position of the myristoyl moiety. The CCLS pulse sequence allows the detection of amide resonances that contain ^{15}N–^{13}C′ pairs. It consists of the acquisition of a control [^{1}H/^{15}N]HSQC ^{13}C′-decoupled spectrum with constant time evolution of the ^{15}N magnetization and a suppression spectrum, where ^{15}N resonances coupled to ^{13}C′ (in this case, the ^{13}C-1 of the myristoyl group) become suppressed. The subtraction of the two spectra results in a subspectrum with only the amide resonances linked to ^{13}C carbonyl carbons detected. For myr(+)p(+)PKA-C, the difference spectrum revealed a single ^{1}H/^{15}N resonance, which corresponded to the G1 amide covalently attached to the myristoyl group (Fig. 1d).

To test the structural integrity and the activity of myr(−)p(+)PKA-C and myr(+)p(+)PKA-C, we carried out kinetic and thermodynamic assays. A summary of these kinetic and thermodynamic parameters is reported in Table 1. In particular, we tested nucleotide binding affinity by ITC measurements and the catalytic phosphorylation efficiency with the standard substrate kemptide. ITC measurements showed that both myr(−)p(+)PKA-C and myr(+)p(+)PKA-C have identical dissociation constants (K_d) for adenosine diphosphate (ADP), with similar thermodynamic properties (Fig. S2). As for the recombinantly expressed myr(+)p(−)PKA-C,[10] the catalytic efficiency for myr(+)p(+)PKA-C and myr(−)p(+)PKA-C is nearly identical, having similar values of k_{cat} (~20 s^{-1}) and K_m (~40 μM).[10] Taken together, the experimental data from CD, thermal melting, phosphorylation kinetics, and nucleotide binding indicate that the *in vitro* myristoylation protocol preserved the overall fold, activity, and nucleotide binding properties of the enzyme.

The [^{1}H/^{15}N]transverse relaxation optimized spectroscopy (TROSY)–HSQC spectra of ADP-bound myr(−)p(+)PKA-C and ADP-bound myr(+)p(+)PKA-C had very similar amide fingerprints, consistent with the identical CD profiles observed. The differences in the amide fingerprint are mainly due to the hydrophobic myristoyl group. This was verified by titrations of MEGA-8 into samples containing ^{15}N-labeled myr(−)p(+)PKA-C and measuring the amide shifts in the TROSY–HSQC NMR spectra. MEGA-8 is a myristoyl group analog, and a crystal structure of myr(−)p(−)PKA-C bound to MEGA-8 showed that it occupied the same hydrophobic pocket as the myristoyl group in myr(+)p(−)PKA-C.[20] The NMR spectrum of MEGA-8-bound myr(−)p(+)PKA-C was nearly superimposable with myr(+)p(+)PKA-C, with only small differences in the extent of changes in chemical shits. Therefore, the assignment myr(+)p(+)PKA-C was facilitated by the comparison with the NMR spectrum of myr(−)PKA-C with MEGA-8-bound myr(−)p(+)PKA-C. A plot of the ^{1}H/^{15}N combined chemical shift perturbations (Δδ) for the presence of the covalently attached myristoyl group or non-covalently bound MEGA-8 is reported in Fig. 2a. The largest changes (Δδ ~ 0.1–0.15 ppm) caused by the myristoyl group are mainly clustered at the hydrophobic pocket of the enzyme, formed between the large lobe and the N-terminal A-helix (Fig. 2b). These perturbations are also present in the E-helix and for several residues

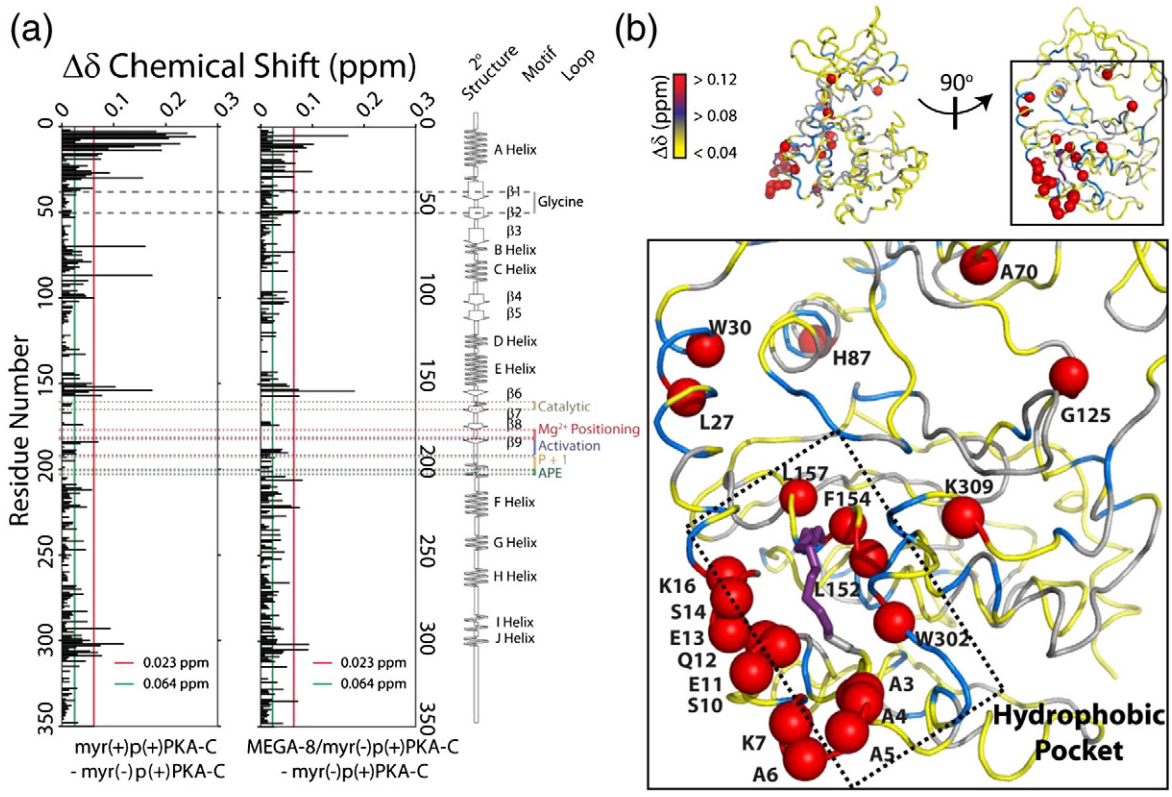

Fig. 2. Mapping the changes upon myristoylation of PKA-C. (a) Chemical shift perturbations (Δδ) *versus* residues upon myristoylation and detergent (MEGA-8) binding. (b) Mapping of Δδ for myristoylation changes on a cartoon representation of PKA-C crystal structure.

that have been predicted to contact the myristoyl group in the crystal structure of myr(+)p(−)PKA-C [Protein Data Bank (PDB) ID: 1CMK[21]] or MEGA-8-bound myr(−)p(−)PKA-C (PDB ID: 1SMH[14]). In addition to local perturbations, significant changes were observed for residues located in helices B and C and near the active site of the enzyme, suggesting long-range allosteric effects of the myristoyl group.

Role of the myristoyl group in membrane association of PKA-C

Previous reports indicated that, in addition to membrane interactions mediated by the myristoyl group, a cluster of basic residues at the N-terminus and large lobe of PKA-C can also facilitate membrane binding.[12,14] To establish the role of the myristoyl group in mediating the interaction with lipid membranes and to determine whether the basic residues alone in PKA-C may facilitate these interactions, we first used intrinsic tryptophan fluorescence. Based on the X-ray crystal structures of myr(+)p(−)PKA-C, at least two tryptophan residues (W30 and W302) would be sensitive to structural changes at the myristoyl hydrophobic pocket of the protein kinase (Fig. S3). In addition, at least six nearby aromatic residues (Phe or Tyr) could affect the tryptophan fluorescence signal in the hydrophobic pocket.[6] Isotropic bicelles composed of 1,2-dimyristoyl-*sn*-glycero-3-phosphocholine (DMPC)/1,2-diheptanoyl-*sn*-glyero-2-phosphocholine (D7PC) ($q = 0.5$ and $c_L \sim 3$–24%) were added stepwise to myr(−)p(+)PKA-C or myr(+)p(+)PKA-C, and their tryptophan fluorescence was measured. Duplicate spectra without PKA-C samples were acquired to subtract any possible changes in the background signal due to the bicelles. The addition of bicelles to myr(−)p(+)PKA-C led to a small enhancement in the intrinsic fluorescence signal measured (Fig. 3a). In contrast, the addition of bicelles to myr(+)p(+)PKA-C led to a fourfold enhancement of the intrinsic fluorescence (Fig. 3b, arrows), consistent with at least one tryptophan of the enzyme being exposed to a less polar environment. Although a 10- to 20-nm blue shift in the fluorescence signal may be expected, this was likely masked by the lack of effects for the majority of tryptophan residues far from the hydrophobic pocket in the enzyme (Fig. S4). The enzyme interaction with isotropic bicelles was further verified by measuring the profile and signal intensity changes in the amide region of NMR spectra (Fig. 3c). Consistent with the intrinsic tryptophan fluorescence measurements, small changes in the profile

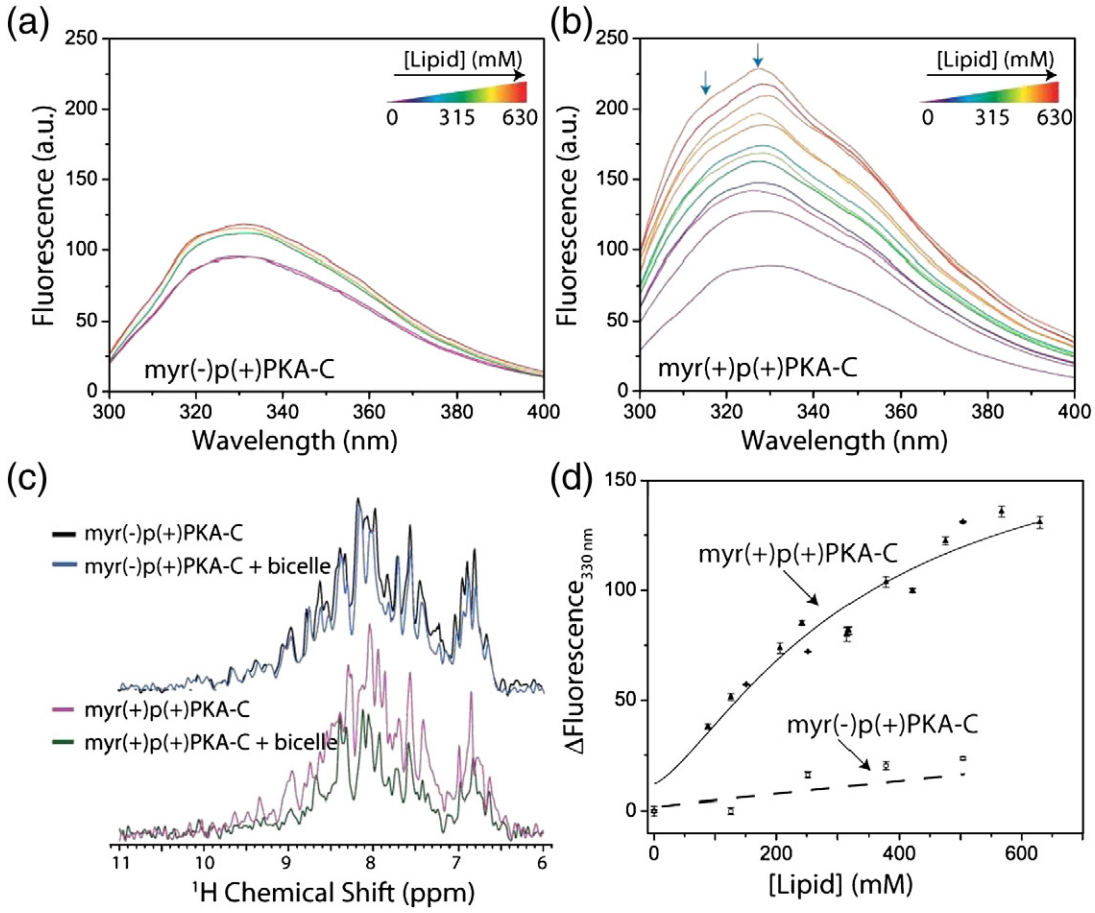

Fig. 3. Membrane interactions of myr(−)p(+)PKA-C and myr(+)p(+)PKA-C. Intrinsic fluorescence spectra as a function of bicelle addition for (a) myr(−)p(+)PKA-C and (b) myr(+)p(+)PKA-C. (c) N-edited 1D ^{1}H NMR spectra for myr(−)p(+)PKA-C and myr(+)p(+)PKA-C showing the signal reduction upon addition of 15% isotropic bicelles. (d) Binding isotherms for both enzymes obtained from intrinsic fluorescence spectra.

and signal intensity of the one-dimensional (1D) ^{1}H spectrum of myr(−)p(+)PKA-C were detected. However, the changes for the myr(+)p(+)PKA-C sample were more drastic upon addition of bicelles. Specifically, the signal intensity decreased by 40–60%. This decrease is consistent with myr(+)p(+)PKA-C binding to the larger bicellar structure, causing a change in rotational correlation time. We fit the bicelle-induced changes in tryptophan fluorescence intensity to a one-site binding model and found a K_d of ~260 mM for myr(+)p(+)PKA-C and ~1200 mM for myr(−)p(+)PKA-C (Fig. 3d). These data indicate that although myr(−)p(+)PKA-C may have some interaction with the membrane surface of bicelles, this interaction is strengthened by the presence of the myristoyl group in myr(+)p(+)PKA-C.

To characterize the lipid interactions at the atomic level, we analyzed amide ^{1}H/^{15}N combined chemical shift perturbations of both myr(−)p(+)PKA-C and myr(+)p(+)PKA-C upon addition of isotropic bicelles. Consistent with the weak binding to bicelles observed by 1D ^{1}H NMR measurements and tryptophan fluorescence changes, the perturbations in the amide fingerprint spectra of ^{15}N-labeled myr(−)p(+)PKA-C with bicelles were small (Fig. 4a and Fig. S4). In contrast, the spectrum of ^{15}N-labeled myr(+)p(+)PKA-C changed more substantially. In particular, the spectrum of myr(+)p(+)PKA-C was drastically attenuated in the presence of bicelles, suggesting a longer rotational correlation time (Fig. 4a). Mapping of the chemical shift perturbations in ^{15}N-labeled myr(+)p(+)PKA-C (Fig. 4b) showed localized changes at the hydrophobic pocket. In addition, long-range allosteric changes in helices B, C, E, F, and J were also present. Interestingly, a cluster of residues (G50, G55, F69, A70, and Y122) near the active site of the enzyme was substantially perturbed. Small changes were detected near conserved residues involved in catalysis, such as the glycine-rich Asp^{184}-Phe^{185}-Gly^{186}, activation, and peptide positioning loops. These changes were propagated as far away as ~30 Å from the hydrophobic pocket of myr(+)p(+)PKA-C, exemplifying an allosteric change within the enzyme upon membrane interaction.

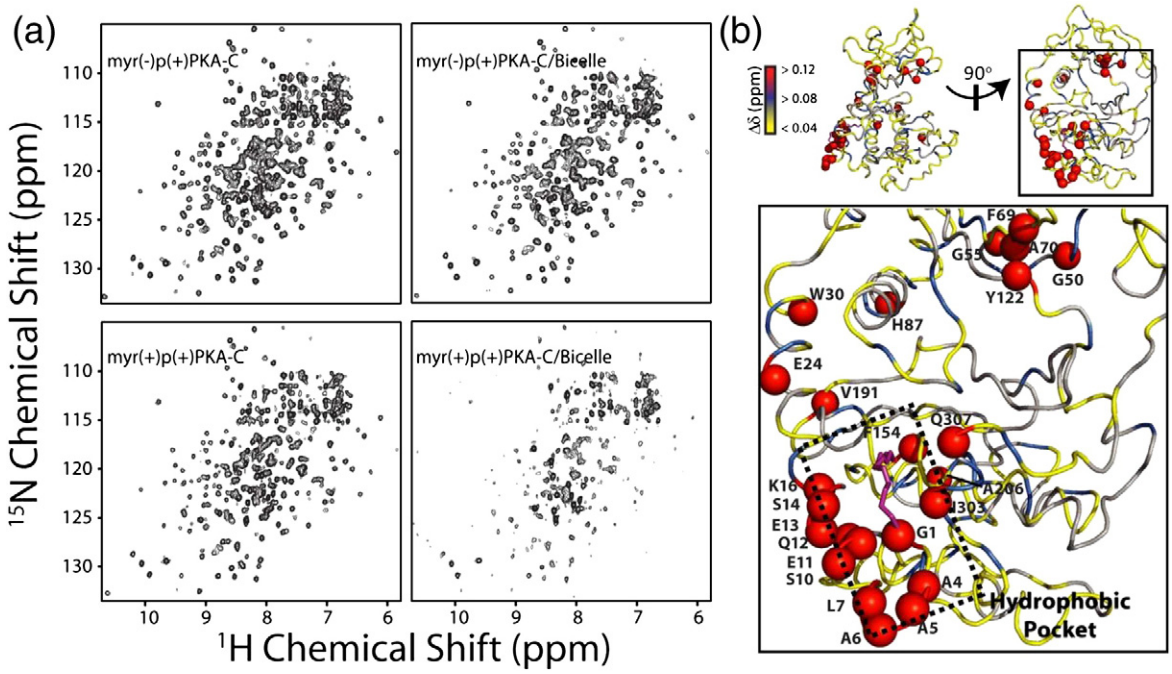

Fig. 4. Atomic details of PKA-C interaction with bicelles. (a) Two-dimensional [^{1}H,^{15}N]HSQC spectra for myr(−)p(+)PKA-C and myr(+)p(+)PKA-C in the presence of 15% isotropic bicelles. (b) Mapping of Δδ for myr(+)p(+)PKA-C upon perturbation with 5% isotropic bicelles showed localized effects on the hydrophobic pocket and allosteric effects, including a group of residues at the active site of the enzyme ~30 Å from the myristoyl group.

Evidence for a conformational switch in myristoylated PKA-C

As suggested by crystallographic data, the conformation of the N-terminus of PKA-C may be sensitive to phosphorylation at S10.[10–13,15,20] Crystal structures of myr(+)p(−)PKA-C containing non-phosphorylated S10 show an ordered α-helix at the N-terminus.[11] On the other hand, a lack of electron density for myr(−)p(+)PKA-C,[22] which is phosphorylated at S10, suggests an unfolded disordered N-terminus. In order to glean insight into how phosphorylation may affect the conformation of the N-terminus, we recorded TROSY–HSQC spectra for PKA-C samples where myristoylation was present or absent [myr(+) or myr(−), respectively] and where phosphorylation was present or absent [p(+) and p(−), respectively]. When data for samples containing isotropic bicelles were included, a clear trend in chemical shift changes was evident for residues in the proximity of the hydrophobic pocket: A3–A6, N289, W302, and A312. At one end of the extreme was the downfield-shifted ^{1}H NMR resonances myr(−)p(+)PKA-C (red resonances, Fig. 5). At the other extreme was the upfield-shifted ^{1}H NMR resonances of myr(+)p(−)PKA-C (black resonances, Fig. 5). The position of these NMR resonances renders an *apparent* two-state equilibrium: downfield ^{1}H NMR resonances suggest a disordered conformation of the N-terminus that is solvent exposed, a state that we termed *myr-out*, while the upfield shifts are consistent with an ordered helical conformation of the N-terminus that is solvent protected, a state that we termed *myr-in*.

A number of samples had chemical shift positions that lie in between the two extremes identified, indicative of fast exchange between these two predominant conformational states. Notably, the membrane-free myristoylated samples (Fig. 5, black and purple resonances) were shifted toward the *myr-out* conformational state in the presence of isotropic bicelles (Fig. 5, dark-blue and light-blue resonances). In addition, all phosphorylated samples (Fig. 5, red, pink, dark-blue, and purple resonances) were shifted toward the *myr-out* state relative to the non-phosphorylated samples (Fig. 5, yellow, green, light-blue, and black resonances). This suggests that myr(+)PKA-C undergoes a conformational equilibrium at its N-terminus, where the amphipathic N-terminal helix can interact with the charged lipid headgroup and a shift to a more unfolded conformation can occur by either phosphorylation at Ser10 or myristoyl interaction with the membrane surface (Fig. S5).

Positioning of the myristoyl group within the lipid bilayer

To verify the extrusion of the myristoyl group of myr(+)p(+)PKA-C out of the hydrophobic pocket and into the lipid bilayer, we reconstituted myr(+)p(+)PKA-C into oriented lipid bicelles composed of

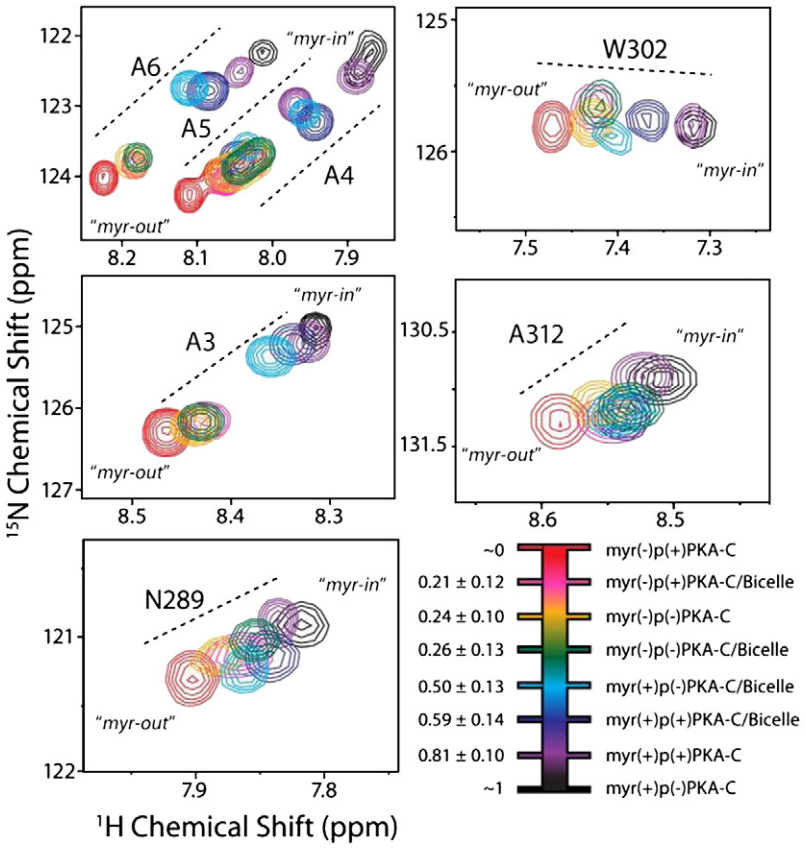

Fig. 5. Conformational switch of myr(+)PKA-C probed by NMR chemical shift analysis. Selected regions of the two-dimensional [^{1}H,^{15}N]HSQC spectra of specific residues undergoing fast conformational exchange between *myr-in* and *myr-out* states. The different colors indicate the various PKA-C species in the absence or presence of phosphorylation, myristoylation, and lipid bicelles. The linear trajectories of the chemical shifts observed between two extremes, corresponding to a *myr-in* state (black resonances) and a *myr-out* state (red resonances), indicate that phosphorylation and interaction with bicelles shift the conformational equilibrium at the N-terminus. Experimental conditions are detailed on Materials and Methods.

DMPC/D7PC (q=3.2 and c_L=10%). [^{2}H]myr(+)p(+)PKA-C, which had ^{2}H labeling only at the myristoyl group, was obtained by incorporating ^{2}H-labeled myristic acid into Myr-CoA. Using ^{2}H DMPC as a reference for the quadrupolar splitting of the acyl chain in the bicelle (and therefore the order and orientation), we first measured the quadrupolar splittings of the lipid bicelles alone (Fig. 6a). A superposition of ^{2}H quadrupole splittings from each of the motionally averaged sites is observed,[12,23] where the outside edges of the spectrum likely correspond to C-2 methylenes (the least motionally averaged sites) and the centermost splitting corresponds to the terminal methyl group (the most motionally averaged site). We found a maximal splitting of ~22.4 kHz for the most restricted methylene carbons in DMPC. On the other hand, [^{2}H]myr(+)p(+)PKA-C free in solution showed no quadrupolar splitting, as expected for a molecule that has no orientation and tumbles isotropically in solution. Upon addition of aligned bicelles, [^{2}H]myr(+)p(+)PKA-C produced a maximal quadrupolar splitting of ~15.8 kHz. This indicates that the myristoyl group has a decreased order parameter relative to the DMPC acyl chain. To describe the topology of the myristoyl group in the bicelle, we fit the data to a model that assumed that the myristoyl group is static [Eq. (4)] or diffuses in a cone [Eq. (5)]. Using the static model, we found that the myristoyl group must be inserted into the bicelle core and is kinked at an angle of ~26° with respect to the bilayer normal (Table 2 and Fig. 6d). Using a model that assumed diffusion in a cone, we again found that the myristoyl group must be inserted into the bicelle core and the acyl chain wobbles in a cone with an amplitude of ~38° with respect to the bilayer normal (Table 2 and Fig. 6e). These results are in agreement with previous data on a myristoylated peptide corresponding to the first 14 residues of PKA-C, which showed an angle of ~30°.[12] Importantly, if the acyl group of myr(+)p(+)PKA-C were resting on the surface of the bilayer (β_{nm}=90°), the quadrupolar coupling would be ≤11 kHz (i.e., $\leq \frac{1}{2}\Delta_{bicelle}$), assuming no additional uniaxial motion on the surface. However, the observed splitting for the myristoyl group is ~15.8 kHz. Although the observed data do not provide the exact location and dynamics of the myristoyl group from either model used, the measurements indicate unequivocally that the myristoyl group must insert into the lipid bilayer.

Discussion

Previous studies indicated that N-myristoylation does not change the phosphorylation kinetics for soluble substrates[10] and eluded that this modification

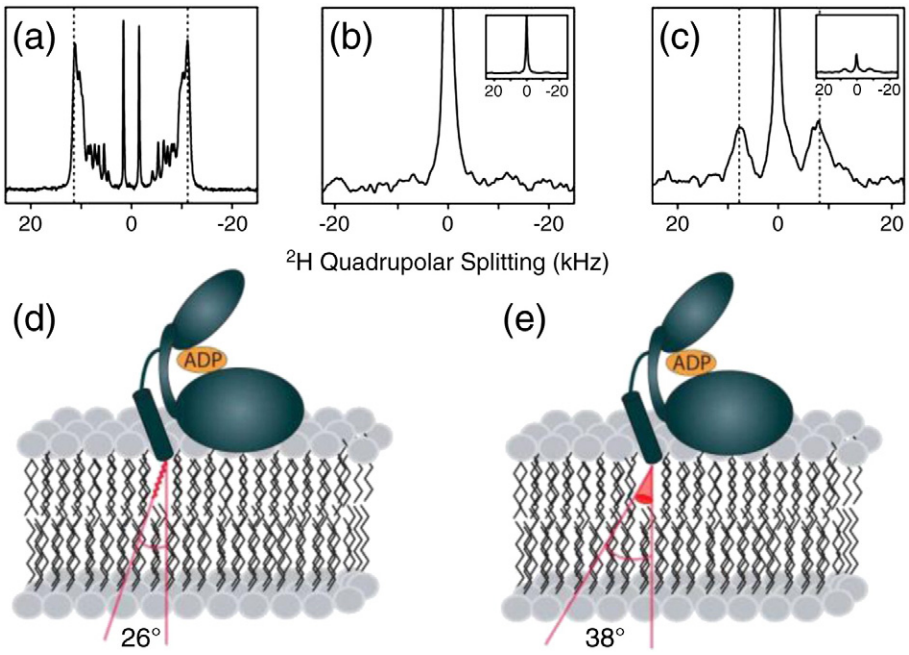

Fig. 6. Probing myr(+)p(+)PKA-C insertion in aligned bicelles using ^{2}H solid-state NMR. (a) ^{2}H spectrum of [$^2H_{54}$] DMPC in aligned bicelles in the absence of myr(+)p(+)PKA-C. ^{2}H spectrum of myr(+)p(+)PKA-C labeled with [$^2H_{27}$] myristic acid in the absence (b) and presence (c) of aligned bicelles. Insertion models of the myristoyl group within the lipid bicelle using static (d) and dynamic (e) models.

changed the membrane localization properties of the enzyme.[12,15] A myristoylation/phosphorylation switch for PKA-C was also hypothesized based on a study that was limited to small peptides corresponding to the N-terminus of the enzyme[13] or to crystal structures that are absent of any membrane environment.[14] The connection for the structural details and localization properties for the full-length protein with the posttranslational modifications of myristoylation/phosphorylation are absent due to difficulty in obtaining N-myristoylated protein that is also phosphorylated. The *in vitro* myristoylation method described here allowed a facile approach to selectively myristoylate a particular phosphoisoform of the enzyme while retaining its functional properties. In this manner, we were able to test how the presence or absence of myristoylation affects interactions with the membrane surface of bicelles, particularly in the context of phosphorylation at S10.

Based on our NMR chemical shift data, myr(+)PKA-C likely undergoes conformational interconversion between two major states: a *myr-in* state, where the myristoyl group is tucked into the hydrophobic pocket of the enzyme, and a *myr-out* state, where the myristoyl group is extruded from the hydrophobic pocket (Fig. 7). The conformations of these major states are best characterized by crystallographic data: the *myr-in* state is best represented by the two additional turns of the N-terminal α-helix of myr(+)p(−)PKA-C, and the *myr-out* state is best represented by the lack of electron density for the first ~12 residues at the N-terminus of myr(−)p(+)PKA-C. The structural features of these two conformational states agree well with the change in thermostability and the ΔC_p between myr(+)p(+)PKA-C and myr(−)p(+)PKA-C that we measured in the current study. However, the NMR chemical shift changes measured allowed us to identify two additional states (Fig. S5) that reflect the concomitant folding and unfolding of the N-terminal helix. This event allows the extrusion of the myristoyl group and its insertion into the membrane core. These states lie along the same path of the two major states and indicate that folding and unfolding of the N-terminal helix is an integral part of the mechanism of the myristoyl switch. Therefore, we propose that myr(+)PKA-C has a highly populated *myr-in* state in the absence of membranes, and a population shift to the *myr-out* state is induced by the presence of a membrane surface (Fig. 7) or phosphorylation at S10. The chemical shift changes in myr(+)p(+)PKA-C and myr(+)p(−)PKA-C

Table 2. Model fitting results from ^{2}H NMR spectroscopy

Sample	Quadrupolar splitting (kHz)	β_{ij}[a] (°)	β_o[b] (°)
Bicelle ([$^2H_{54}$]DMPC)	22.3	—	—
[^{2}H]myr(+)p(+)PKA-C + bicelle	15.8	26	38

[a] Static angle.
[b] Angle for diffusion in a cone.

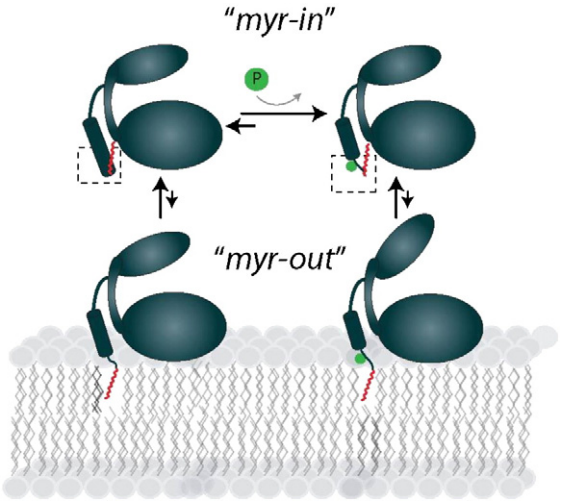

Fig. 7. Proposed model of a myristoyl/phosphorylation conformational switch in PKA-C. PKA-C undergoes conformational interconversion between an N-terminal tucked *myr-in* state and an N-terminal extruded *myr-out* state. Phosphorylation and the presence of membranes cause a shift to a larger population of *myr-out* state that may facilitate the interaction with membranes.

illustrate this point. Residues in the hydrophobic pocket report on a *myr-in* state of ~81% for myr(+)p(+)PKA-C, which shifts to ~59% in the presence of bicelles, whereas phosphorylation appears to shift the *myr-in* state of myr(+)p(−)PKA-C from 100% to ~81% (Fig. 6). X-ray crystallography[11,21] and NMR[24–26] data indicate that membrane-free myr(−)p(+)PKA-C has a highly mobile, unstructured N-terminus. Therefore, the *myr-out* state likely contains an unwound N-terminus, which likely decreases the stability of the enzyme. These dynamics of the *myr-out* conformational state may facilitate lipid binding by exposing both the basic patch and the myristoyl anchor at the N-terminus.

The extrusion of the myristoyl group in the *myr-out* state and its insertion into the hydrocarbon region of the lipid bilayer are supported by ^{2}H NMR measurements. Membrane-free [^{2}H]myr(+)PKA-C showed a completely isotropic peak for the d_{27}-myristoyl group. A dramatic restriction of the myristoyl group dynamics was observed in the presence of anisotropic bicelles, consistent with the myristoyl group inserted into the bicelle core. The data also indicated that the myristoyl group likely assumes some degree of tilt inside the bilayer core. Although we showed evidence that myr(−)PKA-C interacts weakly with the membrane surface of bicelles, the interaction is stronger for myr(+)PKA-C. This underscores the important role of the myristoyl group to localize PKA-C to the membrane and facilitates its interactions with proteins at the interface between the membrane and the aqueous environments.

The ability of myr(+)PKA-C to undergo a population shift to a *myr-out* state is reminiscent of the Ca^{2+}-activated switch proposed for recoverin[27] and other myristoyl-mediated membrane interactions proposed for Ras,[28] guanylate cyclase,[29,30] human immunodeficiency virus 1 Nef, human immunodeficiency virus 1 MA, and ADP-ribosylation factor 1.[23,31–37] However, our data indicate that the role of N-myristoylation of PKA-C differs significantly from that identified for other protein kinases, such as Abl and c-Src.[8,9] For these signaling enzymes, myristoylation does not necessarily coincide with their interactions with cellular membranes; rather, it plays a role in the regulatory mechanism. Our studies show that the myristoyl group of myr(+)PKA-C undergoes a switch-like mechanism that plays a role in localization, specifically, trafficking the protein kinase to membrane surfaces. Therefore, protein kinase myristoylation represents a general control of the function, but the mechanism may be context specific, fine-tuning phosphorylation levels in different cellular compartments. Nonetheless, the *N*-myristoyl/phosphoserine switch might be necessary but not sufficient for effective membrane targeting of the kinase. In fact, the apparent K_d for lipid binding is rather weak compare to similar systems such as MARCKS (*m*yristoylated *a*lanine-*r*ich *C* *k*inase *s*ubstrate).[38] However, PKA-C is exquisitely sensitive to ligand binding,[24–26] and unique changes in the dynamics of the enzyme are widespread depending on the ligand-bound form of PKA-C. Therefore, it is possible that nucleotides, substrates, or inhibitors may provide another avenue to induce a myristoyl switch in PKA-C, similar to the mechanism hypothesized for ARF1.[34,35] AKAPs and the RII subunit may further amplify this signaling and contribute to PKA-C membrane binding and localization.

A previously unidentified aspect from the NMR analysis is the identification of allosteric changes that are distal to the myristoylation pocket. These residues were perturbed upon integration of myristoyl group into the enzyme or when the myristoyl group became extruded from the hydrophobic pocket upon interaction with lipid membranes. These residues represent remote sites that are in allosteric communication with the hydrophobic pocket and may be pivotal in understanding how allostery occurs in this complex enzyme. It is possible that myristoylation constitutes an internal control that modulates function, and these allosteric effects observed for remote residues may reveal new elements to control PKA-C function, as in the case of Bcr–Abl kinase.[39]

In sum, our results provide evidence that the membrane binding motif of myr(+)PKA-C steers the enzyme to the membrane surface, a mechanism that may be controlled by a phosphoserine switch and is independent from AKAPs or RII subunit. Direct

lipid association of myr(+)PKA-C may work in concert with these proteins to insure optimal response to signaling cascades at the lipid interface.

Materials and Methods

Synthesis of Myr-CoA

CoA (free acid) was from Avanti Polar Lipids. Myr-CoA thioester was synthesized, as previously described, with minor modifications to the protocol.[18] Myristic acid (12 mg, 0.052 mmol; MP Biomedicals) and 1,1′-carbonyldiimidazole (8.4 mg, 0.052 mmol; Aldrich) were dissolved in 2 mL dry CH_2Cl_2 and 2 mL dry tetrahydrofuran (THF). The reaction was stirred for 30 min, and the solvents were removed *in vacuo*. The residue was dissolved in 2 mL dry THF, and the solution was added to CoA (20 mg, 0.026 mmol) dissolved in 2 mL of 0.5 M aqueous $NaHCO_3$. The reaction was stirred for 2 h. The formation of Myr-CoA was monitored by reversed-phase HPLC on a C18 column with detection at 280 nm. Myr-CoA has a $T_r = 42.9$ min using a gradient of 0–60% acetonitrile/0.1% trifluoroacetic acid (TFA) (buffer B) over 60 min. THF was removed *in vacuo*, and Myr-CoA was precipitated by dropwise addition of 20% perchloric acid until CO_2 evolution ceased. The precipitate was centrifuged, and the pellet was washed three times with acetone. The acetone was removed, and the pellet was dissolved in double-distilled H_2O. The solute was divided equally between four Eppendorf tubes and lyophilized. Myr-CoA was stored dessicated at −20 °C. Identity was confirmed by ESI-TOF-MS (calculated, 977.3 a.m.u.; found, 977.3 a.m.u.).

In vitro myristoylation of PKA-C by NMT

Recombinant PKA-C and NMT were expressed and purified as previously described.[40] For the myristoylation reaction, myr(−)p(+)PKA-C or myr(−)p(−)PKA-C was dialyzed extensively against buffer A [20 mM KH_2PO_4 (pH 7.4), 90 mM KCl, 1 mM NaN_3, 1 mM $MgCl_2$, and 10 mM sucrose] at 4 °C and concentrated to 150 μM using a centrifugal concentrator (10-kDa cutoff; Millipore). The protein kinase was then diluted to 30 μM in buffer A containing 10 mM ADP and 3 mM 3-[(3-cholamidopropyl) dimethylammonio]-2-hydroxy-1-propanesulfonate, followed by addition of NMT (final concentration of 1.2 μM). The reaction was initiated by addition of 500 μM Myr-CoA from a 12.5-mM aqueous stock at pH 7.4. The reaction mixture was incubated at 24 °C for ~6 h under gentle agitation. After the reaction, the mixture was diluted five times with buffer [20 mM KH_2PO_4 (pH 7.4), 25 mM KCl, 5% (v/v) glycerol, and 1 mM DTT (pH 7.4)] and dialyzed once against the same solution composition at pH 6.5. Separation from residual NMT was achieved by cation exchange on a MonoS column (GE Life Sciences) using a linear gradient from buffer C [20 mM KH_2PO_4 (pH 6.5), 5 mM DTT, and 5% glycerol] into the same buffer containing 1 M KCl (0–8% over 5 min; 8–18% over 66 min). The enzyme product was dialyzed against buffer C with 180 mM KCl, 1 mM NaN_3, 10 mM $MgCl_2$, 10 mM DTT, and 10 mM ADP. The molecular weight of myr(+)p(+)PKA-C was confirmed by ESI mass spectrometry carried out using ESI-TOF-MS. The sample was prepared by desalting on a reversed-phase C18 analytical column (Vydac), using a linear gradient of water/0.1% TFA into acetonitrile/0.1% TFA (0–20% over 20 min, 21–44% over 5 min, and 45–49% over 10 min). For myr(+)p(+)PKA-C, a calculated mass of 40,897 a.m.u. was expected, and 40,896 a.m.u. was found.

Intrinsic fluorescence measurements

Fluorescence spectra were recorded on a Varian Cary Eclipse fluorescence spectrophotometer. The excitation wavelength was set to 280 nm, and emission was recorded from 300 to 400 nm. The slit width was set to 10 nm (5 nm) for the excitation (emission). The scan rate was 120 nm/min, with a 1-nm data interval and 0.5 s of averaging time. The protein concentration was 0.33 μM in 20 mM KH_2PO_4 (pH 6.5), 180 mM KCl, 100 nM ethylene glycol bis(β-aminoethyl ether) *N,N′*-tetraacetic acid, and 5% (v/v) glycerol. A stock solution of isotropic bicelles [$q = 0.5$, 40% (w/v) DMPC/D7PC] was prepared in the same buffer. All the bicelle samples were prepared separately, and the fluorescence spectra were recorded 5 min after addition. All experiments were performed in triplicate. Fluorescence spectra were corrected for the blank. The blue shift observed when the bicelles were added was most dominant at 315 nm. The increase in fluorescence was fit to a one-site binding model using Origin 7.0 (Microcal).

ITC and DSC

For ITC measurements, the enzyme buffer was exchanged into ITC buffer containing 50 mM Mops (pH 7.0), 5 mM $MgCl_2$, and 1 mM DTT. The enzyme was concentrated by filtration to ~23 μM at pH 6.5. The injectant consisted of 670 μM ADP in ITC buffer. Samples were degassed for ~10 min prior to titration of the ligand. ITC was carried out on a Microcal MCS-ITC at 27 °C with a stirring rate of 400 r.p.m. The titrations consisted of an initial 2-μL injection of ADP, followed by twenty 10-μL injections. An initial delay of 60-s and 300-s waiting time between each consecutive injection was used. The binding curves were fit to a one-site binding model using Origin 7.0 (Microcal). The curves were corrected for the heat of dilution, which was determined by separate blank titrations of ADP into ITC buffer.

For DSC measurements, samples were prepared in DSC buffer [20 mM KH_2PO_4 (pH 6.5), 150 mM KCl, 10 mM $MgCl_2$, 10 mM DTT, and 1 mM NaN_3] to a concentration of ~25 μM. Both samples were degassed with stirring for 5 min in a ThermoVac (Microcal). DSC measurements were carried out on a Microcal VP-DSC instrument over a temperature range of 20–60 °C, a scan rate of 90 °C/h, and a prescan delay of 15 min. Two scans were carried out with each sample, which verified the irreversibility of the transition. Data analysis was carried out in Origin (Microcal). Reference scans were obtained using reference buffer and were subtracted during data analysis.

Thermostability by CD spectroscopy

Samples consisted of 10 μM protein kinase in 5 mM KH_2PO_4 (pH 6.5), 45 mM KCl, 1 mM NaN_3, and 300 μM MgADP. Far-UV (190–260 nm) CD spectra were obtained on

a Jasco J-715 spectropolarimeter. The samples were measured in a 1-mm dichroically neutral quartz cuvette with a 1-mm bandwidth, a 2-s time constant, of 20 nm/min scan speed, and an average of two scans with background signal correction. After acquisition of the far-UV profile, the samples were heated to 65 °C at 3 °C/min (10-s equilibration), and the signal at 222 nm was measured as a reporter of thermal melting. Data were fit to a two-state sigmoidal unfolding model with Origin 8.0 (Microcal), and the midpoint of the curve was taken as the melting temperature (T_m).

NMR spectroscopy

NMR experiments were carried out on a Varian Inova spectrometer operating at 599.71 MHz and equipped with an HCN probe. Enzyme samples were prepared in 20 mM KH_2PO_4, 180 mM KCl, 1 mM NaN_3, 10 mM DTT, 10 mM ADP, 10 mM $MgCl_2$, 5% (v/v) glycerol, and 5% (v/v) D_2O (pH 6.5). The concentrations of the samples were ~0.1–0.3 mM. To confirm the N-terminal linkage between the myristic acid and the protein, we used myristic acid with ^{13}C incorporated specifically at the carbonyl position to synthesize Myr-CoA for *in vitro* reactions. PKA-C (uniformly labeled with ^{15}N) was then myristoylated enzymatically by NMT as described previously. To detect the linkage, we used the carbonyl carbon label selective [$^1H/^{15}N$]CCLS–HSQC experiment,[19] which detects ^{15}N-labeled amide groups covalently linked to ^{13}C-labeled carbonyl groups. For membrane binding studies, we prepared DMPC/D7PC isotropic bicelles ($q=0.5$ and $c_L=40\%$ for stock solutions). The NMR data were processed and visualized using NMRPipe[41] and SPARKY.[42] Backbone resonance assignments were performed by (1) comparison of the myr(+)p(+)PKA-C fingerprint with those of myr(−)p(+)PKA-C,[43] (2) following the NMR chemical shifts during titrations of myr(−)p(+)PKA-C with the myristoyl analog MEGA-8, and (3) additional resolution provided by ^{15}N selectively labeled samples (Glu, Lys, and Ala residues) of myr(+)p(+)PKA-C (Fig. S6). Chemical shift perturbations from the NMR titrations were measured using combined chemical shifts according to the following equation:

$$\Delta\delta = \sqrt{\Delta\delta_H^2 + (0.154 \times \Delta\delta_N)^2} \quad (1)$$

where $\Delta\delta$ is the combined chemical shift, and $\Delta\delta_H$ and $\Delta\delta_N$ are the differences of ^1H and ^{15}N chemical shifts, respectively, between the two different isoforms or the first and last points of titrations. Populations of the *myr-in* state ($p_{myr\text{-}in}$) were quantified using:

$$p_{myr-in} = \frac{\Omega_x - \Omega_{myr-out}}{\Omega_{myr-in} - \Omega_{myr-out}} \quad (2)$$

where Ω_x, $\Omega_{myr\text{-}out}$, and $\Omega_{myr\text{-}in}$ are the chemical shift of sample *X*, myr(−)p(+)PKA-C, and myr(+)p(−)PKA-C, respectively. The mean of $p_{myr\text{-}in}$ was determined from seven resonances distributed within 12 Å from the myristoyl group in PDB ID: 1CMK.

^2H solid-state NMR spectroscopy

Deuterated myristic acid ([^2H]myr) was used to prepare [^2H]myr(+)p(+)PKA-C for the measurement of quadrupolar splitting in the presence or absence of aligned bicelles (DMPC/D7PC, $q=3.2$) by solid-state NMR. NMR samples were prepared in 20 mM KH_2PO_4 (pH 6.5), 180 mM KCl, 1 mM NaN_3, 10 mM DTT, 20 mM ADP, 20 mM $MgCl_2$, and 5% (v/v) glycerol in deuterium-depleted water. Stock bicelle solutions ($c_L=30\%$) were titrated into an enzyme solution on ice to obtain a final concentration of 600 μM myr(+)p(+)PKA-C and a c_L of 10%. Quadrupolar splittings of DMPC were performed on a bicelle solution containing 2% (v/v) [$^2H_{54}$]DMPC of the total DMPC present. All ^2H experiments were recorded at a ^2H resonance frequency of 107.4 MHz. Samples were initially at 5 °C, gradually warmed to 27 °C over 10 min, and equilibrated for 30 min. The bicelle alignment was checked by ^{31}P NMR spectroscopy. A quadrupolar echo sequence, $(\pi/2)$-τ_1-$(\pi/2)$-τ_2, was used to measure the ^2H quadrupolar splitting. The spectra of myr(+)p(+)PKA-C in the presence and absence of bicelles were acquired with 40,000 scans each.

The bicellar composition used in this study has a negative order parameter such that the bilayer normal is oriented perpendicular to the magnetic field. The observed quadrupolar splitting (Δ) for a methylene deuteron in an alkyl chain is given by the following relationship:[44]

$$\Delta = \Delta_p S_{n'l} S_{n'n} S_{nm} S_{mp} \quad (3)$$

where $\Delta_p = \frac{3}{2} e^2 qQ / h = 168$ kHz, and $S_{ij} = \frac{1}{2}\langle 3\cos^2 \beta_{ij} - 1\rangle$ is the orientational order parameter that links the coordinate axes *i* and *j* to one another. This requires obtaining the average orientation of the bicelle normal (n') with respect to the magnetic field in the laboratory frame ($\beta_{n'l}$), the angle between the average bilayer normal and the instantaneous (n) or local bilayer normal ($\beta_{n'n}$), the orientation of a molecular axis (m) with respect to n (β_{nm}), and the local angel between the molecular axis and the principal axis (p) of the quadrupolar tensor along the CD bond (β_{mp}). The expression in Eq. (3) can be simplified by dividing the splitting of the myristoylated sample by that of the bicelle:

$$\frac{\Delta_{myristoyl}}{\Delta_{bicelle}} = S_{nm} \quad (4)$$

The equation above can be fit to extract a static angle or by assuming the diffusion-in-a-cone model shown in Eq. (5):

$$S_{nm} = \frac{1}{2}\cos^2 \beta_0 (\cos \beta_0 + 1) \quad (5)$$

Supplementary materials related to this article can be found online at doi:10.1016/j.jmb.2011.06.034

Acknowledgements

The authors would like to acknowledge Susan Taylor for many helpful discussions. This work was supported by the National Institutes of Health (GM072701 and HL080081 to G.V. and T32DE007288 to L.R.M.) and the American Heart Association (09PRE2080017 to E.M.). NMR data

were collected at the University of Minnesota NMR Facility (National Science Foundation BIR-961477).

References

1. Walsh, D. A., Perkins, J. P. & Krebs, E. G. (1968). An adenosine 3′,5′-monophosphate-dependant protein kinase from rabbit skeletal muscle. *J. Biol. Chem.* **243**, 3763–3765.
2. Shabb, J. B. (2001). Physiological substrates of cAMP-dependent protein kinase. *Chem. Rev.* **101**, 2381–2411.
3. Knighton, D. R., Zheng, J. H., Ten Eyck, L. F., Ashford, V. A., Xuong, N. H., Taylor, S. S. & Sowadski, J. M. (1991). Crystal structure of the catalytic subunit of cyclic adenosine monophosphate-dependent protein kinase. *Science*, **253**, 407–414.
4. Carnegie, G. K., Means, C. K. & Scott, J. D. (2009). A-kinase anchoring proteins: from protein complexes to physiology and disease. *IUBMB Life*, **61**, 394–406.
5. Walsh, D. A., Ashby, C. D., Gonzalez, C., Calkins, D. & Fischer, E. H. (1971). Krebs EG: purification and characterization of a protein inhibitor of adenosine 3′,5′-monophosphate-dependent protein kinases. *J. Biol. Chem.* **246**, 1977–1985.
6. Johnson, D. A., Akamine, P., Radzio-Andzelm, E., Madhusudan, M. & Taylor, S. S. (2001). Dynamics of cAMP-dependent protein kinase. *Chem. Rev.* **101**, 2243–2270.
7. Boutin, J. A. (1997). Myristoylation. *Cell. Signalling*, **9**, 15–35.
8. Hantschel, O., Nagar, B., Guettler, S., Kretzschmar, J., Dorey, K., Kuriyan, J. & Superti-Furga, G. (2003). A myristoyl/phosphotyrosine switch regulates c-Abl. *Cell*, **112**, 845–857.
9. Patwardhan, P. & Resh, M. D. (2010). Myristoylation and membrane binding regulate c-Src stability and kinase activity. *Mol. Cell. Biol.* **30**, 4094–4107.
10. Yonemoto, W., McGlone, M. L. & Taylor, S. S. (1993). N-myristoylation of the catalytic subunit of cAMP-dependent protein kinase conveys structural stability. *J. Biol. Chem.* **268**, 2348–2352.
11. Zheng, J., Knighton, D. R., Nguyen, H. X., Taylor, S. S., Sowadski, J. M. & Ten Eyck, L. F. (1993). Crystal structures of the myristylated catalytic subunit of cAMP-dependent protein kinase reveal open and closed conformations. *Protein Sci.* **2**, 1559–1573.
12. Struppe, J., Komives, E. A., Taylor, S. S. & Vold, R. R. (1998). ^{2}H NMR studies of a myristoylated peptide in neutral and acidic phospholipid bicelles. *Biochemistry*, **37**, 15523–15527.
13. Tholey, A., Pipkorn, R., Bossemeyer, D., Kinzel, V. & Reed, J. (2001). Influence of myristoylation, phosphorylation, and deamidation on the structural behavior of the N-terminus of the catalytic subunit of cAMP-dependent protein kinase. *Biochemistry*, **40**, 225–231.
14. Breitenlechner, C. B., Engh, R. A., Huber, R., Kinzel, V., Bossemeyer, D. & Gassel, M. (2004). The typically disordered N-terminus of PKA can fold as a helix and project the myristoylation site into solution. *Biochemistry*, **43**, 7743–7749.
15. Gangal, M., Clifford, T., Deich, J., Chen, X., Taylor, S. S. & Johnson, D. A. (1999). Mobilization of the A-kinase *N*-myristate through an isoform-specific intermolecular switch. *Proc. Natl Acad. Sci. USA*, **96**, 12394–12399.
16. Duronio, R., Jackson-Machelski, E., Heuckeroth, R. O., Olins, P. O., Devine, C. S., Yonemoto, W. *et al.* (1990). Protein N-myristoylation in *Escherichia coli*: reconstitution of a eukaryotic protein modification in bacteria. *Proc. Natl Acad. Sci. USA*, **87**, 1506–1510.
17. Yonemoto, W. M., McGlone, M. L., Slice, L. W. & Taylor, S. S. (1991). Prokaryotic expression of catalytic subunit of adenosine cyclic monophosphate-dependent protein kinase. *Methods Enzymol.* **200**, 581–596.
18. Heal, W. P., Wickramasinghe, S. R., Bowyer, P. W., Holder, A. A., Smith, D. F., Leatherbarrow, R. J. & Tate, E. W. (2008). Site-specific N-terminal labelling of proteins *in vitro* and *in vivo* using *N*-myristoyltransferase and bioorthogonal ligation chemistry. *Chem. Commun. (Cambridge)*,, 480–482.
19. Tonelli, M., Masterson, L. R., Hallenga, K., Veglia, G. & Markley, J. L. (2007). Carbonyl carbon label selective (CCLS) ^{1}H–^{15}N HSQC experiment for improved detection of backbone ^{13}C–^{15}N cross peaks in larger proteins. *J. Biomol. NMR*, **39**, 177–185.
20. Sowadski, J. M., Ellis, C. A. & Madhusudan (1996). Detergent binding to unmyristylated protein kinase A. Structure implications for the role of myristate. *J. Bioenerg. Biomembr.* **28**, 7–12.
21. Zheng, J., Knighton, D. R., Ten Eyck, L. F., Karlsson, R., Xuong, N., Taylor, S. S. & Sowadski, J. M. (1993). Crystal structure of the catalytic subunit of cAMP-dependent protein kinase complexed with magnesium-ATP and peptide inhibitor. *Biochemistry*, **32**, 2154–2161.
22. Knighton, D. R., Zheng, J., Eyck, L. F. T., Xuong, N. H., Taylor, S. S. & Sowadski, J. M. (1991). Structure of a peptide inhibitor bound to the catalytic subunit of cyclic adenosine monophosphate-dependent protein kinase. *Science*, **253**, 414–420.
23. Valentine, K. G., Mesleh, M. F., Opella, S. J., Ikura, M. & Ames, J. B. (2003). Structure, topology, and dynamics of myristoylated recoverin bound to phospholipid bilayers. *Biochemistry*, **42**, 6333–6340.
24. Masterson, L. R., Mascioni, A., Traaseth, N. J., Taylor, S. S. & Veglia, G. (2008). Allosteric cooperativity in protein kinase A. *Proc. Natl Acad. Sci. USA*, **105**, 506–511.
25. Masterson, L. R., Cheng, C., Yu, T., Tonelli, M., Kornev, A. P., Taylor, S. S. & Veglia, G. (2010). Dynamics connect substrate recognition to catalysis in protein kinase A. *Nat. Chem. Biol.* **6**, 821–828.
26. Masterson, L. R., Shi, L., Metcalfe, E., Gao, J., Taylor, S. S. & Veglia, G. (2011). Dynamically committed, uncommitted, and quenched states encoded in protein kinase A revealed by NMR spectroscopy. *Proc. Natl Acad. Sci. USA*, **108**, 6969–6974.
27. Ames, J. B., Ishima, R., Tanaka, T., Gordon, J. I., Stryer, L. & Ikura, M. (1997). Molecular mechanics of calcium–myristoyl switches. *Nature*, **389**, 198–202.
28. Vogel, A., Reuther, G., Roark, M. B., Tan, K. T., Waldmann, H., Feller, S. E. & Huster, D. (2010). Backbone conformational flexibility of the lipid modified membrane anchor of the human N-Ras protein investigated by solid-state NMR and molecular dynamics simulation. *Biochim. Biophys. Acta*, **1798**, 275–285.

29. Theisgen, S., Scheidt, H. A., Magalhaes, A., Bonagamba, T. J. & Huster, D. (2010). A solid-state NMR study of the structure and dynamics of the myristoylated N-terminus of the guanylate cyclase-activating protein-2. *Biochim. Biophys. Acta*, **1798**, 266–274, doi: 10.1016/j.bbamem.2009.06.028.
30. Theisgen, S., Thomas, L., Schroder, T., Lange, C., Kovermann, M., Balbach, J. & Huster, D. (2011). The presence of membranes or micelles induces structural changes of the myristoylated guanylate-cyclase activating protein-2. *Eur. Biophys. J.* **40**, 565–576.
31. Jeromin, A., Muralidhar, D., Parameswaran, M. N., Roder, J., Fairwell, T., Scarlata, S. *et al.* (2004). N-terminal myristoylation regulates calcium-induced conformational changes in neuronal calcium sensor-1. *J. Biol. Chem.* **279**, 27158–27167.
32. Provitera, P., El-Maghrabi, R. & Scarlata, S. (2006). The effect of HIV-1 Gag myristoylation on membrane binding. *Biophys. Chem.* **119**, 23–32.
33. Losonczi, J. A., Tian, F. & Prestegard, J. H. (2000). Nuclear magnetic resonance studies of the N-terminal fragment of adenosine diphosphate ribosylation factor 1 in micelles and bicelles: influence of N-myristoylation. *Biochemistry*, **39**, 3804–3816.
34. Liu, Y., Kahn, R. A. & Prestegard, J. H. (2009). Structure and membrane interaction of myristoylated ARF1. *Structure*, **17**, 79–87.
35. Liu, Y., Kahn, R. A. & Prestegard, J. H. (2010). Dynamic structure of membrane-anchored Arf·GTP. *Nat. Struct. Mol. Biol.* **17**, 876–881.
36. Saad, J. S., Miller, J., Tai, J., Kim, A., Ghanam, R. H. & Summers, M. F. (2006). Structural basis for targeting HIV-1 Gag proteins to the plasma membrane for virus assembly. *Proc. Natl Acad. Sci. USA*, **103**, 11364–11369.
37. Saad, J. S., Ablan, S. D., Ghanam, R. H., Kim, A., Andrews, K., Nagashima, K. *et al.* (2008). Structure of the myristylated human immunodeficiency virus type 2 matrix protein and the role of phosphatidylinositol-(4,5)-bisphosphate in membrane targeting. *J. Mol. Biol.* **382**, 434–447.
38. Vergeres, G. & Ramsden, J. J. (1998). Binding of MARCKS (myristoylated alanine-rich C kinase substrate)-related protein (MRP) to vesicular phospholipid membranes. *Biochem. J.* **330**, 5–11.
39. Zhang, J., Adrian, F. J., Jahnke, W., Cowan-Jacob, S. W., Li, A. G., Iacob, R. E. *et al.* (2010). Targeting Bcr–Abl by combining allosteric with ATP-binding-site inhibitors. *Nature*, **463**, 501–506.
40. Cook, L. L., Stine, K. E. & Reiter, L. W. (1984). Tin distribution in adult rat tissue after exposure to trimethyltin and triethyltin. *Toxicol. Appl. Pharmacol.* **76**, 344–348.
41. Delaglio, F., Grzesiek, S., Vuister, G. W., Zhu, G., Pfeifer, J. & Bax, A. (1995). NMRPipe: a multidimensional spectral processing system based on UNIX pipes. *J. Biomol. NMR*, **6**, 277–293.
42. Goddard, T. D. & Kneller, D. G. (1999). *SPARKY 3.* University of California, San Francisco, San Francisco, CA.
43. Masterson, L. R., Shi, L., Tonelli, M., Mascioni, A., Mueller, M. M. & Veglia, G. (2009). Backbone NMR resonance assignment of the catalytic subunit of cAMP-dependent protein kinase A in complex with AMP-PNP. *Biomol. NMR Assign.* **3**, 115–117.
44. Seelig, J. (1977). Deuterium magnetic resonance: theory and application to lipid membranes. *Q. Rev. Biophys.* **10**, 353–418.